



Figure 2:  $0.5 < i_{DC1}/i_{DC2} < 2$ .

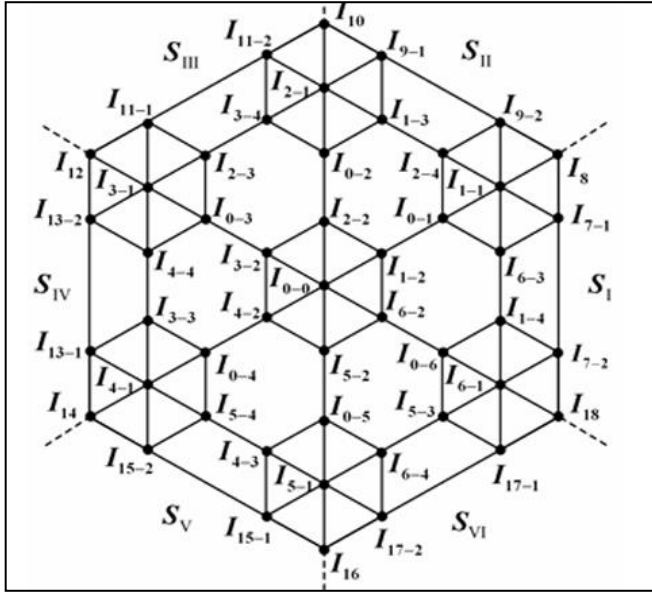


Figure 3:  $(i_{DC1}/i_{DC2} < 0.5)$  or  $(i_{DC1}/i_{DC2} > 2)$ .

### II METHOD 1: IDENTIFYING CLOSEST SWITCHING STATE VECTORS

The CFI unit carrying higher DC-link current is designated as CFI-1, while the other unit is designated as CFI-2. Each major sector ( $S_I$ – $S_{VI}$ ) contains 13 switching state vector positions and is further subdivided into 25 minor sectors.

### III METHOD 2: SELECTION OF SWITCHING STATE VECTORS TO ELIMINATE LOW-FREQUENCY PULSATION

Table 1: Specific switching state vectors are selected for both major and minor sectors under Method 1

Major sector	Minor sector	Switching state vector			Switching states sequence						Number of switch transitions					
		$x$	$y$	$z$	$\frac{T_z}{4}$	-	$T_x$	-	$\frac{T_x}{2}$	-	$T_y$	-	$\frac{T_x}{4}$	CFI-1	CFI-2	Total
	$S_1$	$I_{p-2}$	$I_{q-2}$	$I_{0-0}$	$(i_m, i_m)$	-	$(i_m, i_p)$	-	$(i_m, i_m)$	-	$(i_m, i_q)$	-	$(i_m, i_m)$	0	8	8
	$S_2$	$I_{p-2}$	$I_{q-2}$	$I_{0-p}$	$(i_p, i_w)$	-	$(i_m, i_p)$	-	$(i_p, i_w)$	-	$(i_p, i_q)$	-	$(i_p, i_w)$	8	16	24
	$S_3$	$I_{p-2}$	$I_{q-2}$	$I_{0-q}$	$(i_q, i_n)$	-	$(i_m, i_p)$	-	$(i_q, i_n)$	-	$(i_m, i_q)$	-	$(i_q, i_n)$	8	16	24
	$S_4$	$I_{p-2}$	$I_{q-2}$	$I_{0-p}$	$(i_p, i_w)$	-	$(i_m, i_p)$	-	$(i_p, i_w)$	-	$(i_m, i_q)$	-	$(i_p, i_w)$	8	16	24
	$S_5$	$I_{p-2}$	$I_{q-2}$	$I_{0-q}$	$(i_q, i_n)$	-	$(i_m, i_p)$	-	$(i_q, i_n)$	-	$(i_m, i_q)$	-	$(i_q, i_n)$	8	16	24
	$S_6$	$I_{0-p}$	$I_{0-q}$	$I_{p-2}$	$(i_m, i_p)$	-	$(i_p, i_w)$	-	$(i_m, i_p)$	-	$(i_q, i_n)$	-	$(i_m, i_p)$	8	16	24
	$S_7$	$I_{0-p}$	$I_{0-q}$	$I_{q-2}$	$(i_m, i_q)$	-	$(i_p, i_w)$	-	$(i_m, i_q)$	-	$(i_q, i_n)$	-	$(i_m, i_q)$	8	16	24
	$S_8$	$I_{0-p}$	$I_{0-q}$	$I_{q-4}$	$(i_p, i_v)$	-	$(i_p, i_w)$	-	$(i_p, i_v)$	-	$(i_q, i_n)$	-	$(i_p, i_v)$	4	12	16
	$S_9$	$I_{0-p}$	$I_{0-q}$	$I_{p-3}$	$(i_q, i_u)$	-	$(i_p, i_w)$	-	$(i_q, i_u)$	-	$(i_q, i_n)$	-	$(i_q, i_u)$	4	12	16
	$S_{10}$	$I_{p-1}$	$I_{q-4}$	$I_{0-p}$	$(i_p, i_w)$	-	$(i_p, i_m)$	-	$(i_p, i_w)$	-	$(i_p, i_v)$	-	$(i_p, i_w)$	0	8	8
	$S_{11}$	$I_{0-p}$	$I_{0-q}$	$I_{q-4}$	$(i_p, i_v)$	-	$(i_p, i_w)$	-	$(i_p, i_v)$	-	$(i_q, i_n)$	-	$(i_p, i_v)$	4	12	16
	$S_{12}$	$I_{q-4}$	$I_{p-3}$	$I_{0-p}$	$(i_p, i_w)$	-	$(i_p, i_v)$	-	$(i_p, i_w)$	-	$(i_q, i_n)$	-	$(i_p, i_w)$	4	12	16
$S_M$	$S_{13}$	$I_{q-4}$	$I_{p-3}$	$I_{0-q}$	$(i_q, i_n)$	-	$(i_p, i_v)$	-	$(i_q, i_n)$	-	$(i_q, i_u)$	-	$(i_q, i_n)$	4	12	16
	$S_{14}$	$I_{0-p}$	$I_{0-q}$	$I_{p-3}$	$(i_q, i_u)$	-	$(i_p, i_w)$	-	$(i_q, i_u)$	-	$(i_q, i_n)$	-	$(i_q, i_u)$	4	12	16
	$S_{15}$	$I_{p-3}$	$I_{q-1}$	$I_{0-q}$	$(i_q, i_n)$	-	$(i_q, i_u)$	-	$(i_q, i_n)$	-	$(i_q, i_m)$	-	$(i_q, i_n)$	0	8	8
	$S_{16}$	$I_r$	$I_s-2$	$I_{p-1}$	$(i_p, i_m)$	-	$(i_p, i_p)$	-	$(i_p, i_m)$	-	$(i_p, i_q)$	-	$(i_p, i_m)$	0	8	8
	$S_{17}$	$I_{p-1}$	$I_{q-4}$	$I_s-2$	$(i_p, i_q)$	-	$(i_p, i_m)$	-	$(i_p, i_q)$	-	$(i_p, i_v)$	-	$(i_p, i_q)$	0	8	8
	$S_{18}$	$I_s-2$	$I_s-1$	$I_{q-4}$	$(i_p, i_v)$	-	$(i_p, i_q)$	-	$(i_p, i_v)$	-	$(i_p, i_p)$	-	$(i_p, i_v)$	4	12	16
	$S_{19}$	$I_s-2$	$I_s-1$	$I_{q-4}$	$(i_p, i_v)$	-	$(i_p, i_q)$	-	$(i_p, i_v)$	-	$(i_q, i_p)$	-	$(i_p, i_v)$	4	12	16
	$S_{20}$	$I_{q-4}$	$I_{p-3}$	$I_s-2$	$(i_p, i_q)$	-	$(i_p, i_v)$	-	$(i_p, i_q)$	-	$(i_q, i_u)$	-	$(i_p, i_q)$	4	12	16
	$S_{21}$	$I_{q-4}$	$I_{p-3}$	$I_s-1$	$(i_q, i_p)$	-	$(i_p, i_v)$	-	$(i_q, i_p)$	-	$(i_q, i_u)$	-	$(i_q, i_p)$	4	12	16
	$S_{22}$	$I_s-2$	$I_s-1$	$I_{p-3}$	$(i_q, i_u)$	-	$(i_p, i_q)$	-	$(i_q, i_u)$	-	$(i_q, i_p)$	-	$(i_q, i_u)$	4	12	16
	$S_{23}$	$I_s-2$	$I_s-1$	$I_{p-3}$	$(i_q, i_u)$	-	$(i_p, i_q)$	-	$(i_q, i_u)$	-	$(i_q, i_p)$	-	$(i_q, i_u)$	4	12	16
	$S_{24}$	$I_{p-3}$	$I_{q-1}$	$I_s-1$	$(i_q, i_p)$	-	$(i_q, i_u)$	-	$(i_q, i_p)$	-	$(i_q, i_m)$	-	$(i_q, i_p)$	0	8	8
	$S_{25}$	$I_s-1$	$I_t$	$I_{q-1}$	$(i_q, i_m)$	-	$(i_q, i_p)$	-	$(i_q, i_m)$	-	$(i_q, i_q)$	-	$(i_q, i_m)$	0	8	8

The method eliminates low-frequency pulsations in  $v_{DC1}$  and  $v_{DC2}$  by avoiding specific switching state vectors in certain sectors. Despite this, the output current quality remains consistent, using 9 specific state vectors per major sector, unlike Method 1, and ensuring proper time-sharing between selected switching states.

Vectors  $I_{6-1}$ ,  $I_{6-2}$ ,  $I_{7-1}$ ,  $I_{7-2}$ ,  $I_8$ ,  $I_{18}$ ,  $I_{0-0}$ ,  $I_{1-1}$ ,  $I_{1-2}$  are used in major sector  $S_I$  and active periods for these vectors are,  $T_{6-1}$ ,  $T_{6-2}$ ,  $T_{7-1}$ ,  $T_{7-2}$ ,  $T_8$ ,  $T_{18}$ ,  $T_{0-0}$ ,  $T_{1-1}$ ,  $T_{1-2}$  respectively. If  $T_{6-1} = T_{6-2}$ ,  $T_{1-1} = T_{1-2}$ , and  $T_{7-1} = T_{7-2}$ . The average DC-link voltage over each switching period can be calculated using the following formula,

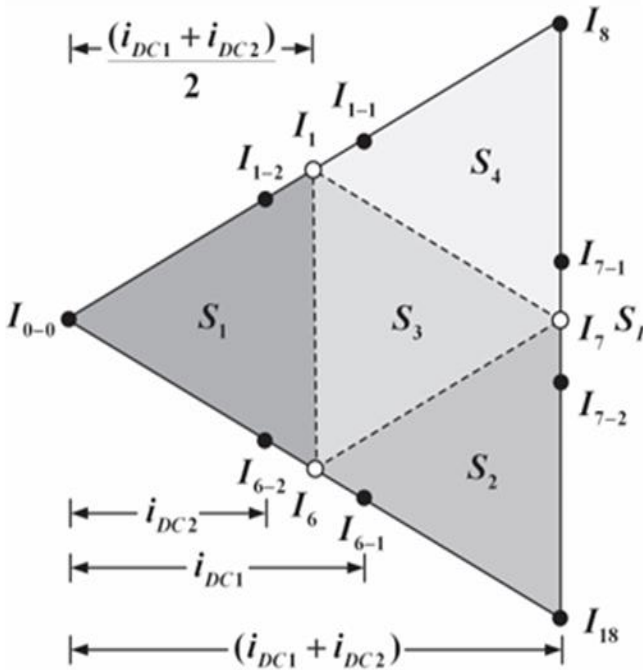
$$V_{DC1} = V_{DC2} = 1.5m V_{ph} \cos\phi$$

where,  $V_{ph}$  = phase voltage,  $m$  = modulation index &  $\cos\phi$  = power factor.

The average DC-link voltage remains constant over each switching period, eliminating low frequency pulsations in  $v_{DC1}$  and  $v_{DC2}$ . A small L-C filter is used to eliminate the switching frequency component and achieve a ripple-free, constant voltage at the DC-DC converter output.

The reference space vector position is determined within minor sectors  $S_1$  to  $S_4$ , bounded by fictitious state vector positions  $I_1$ ,  $I_6$ , and  $I_7$  in major sector  $S_I$ , as shown in Fig. 4

Figure 4: Switching State Vector Alignment



The reference space vector in minor sector S4 is realized with switching state vectors I8, I7-1, I7-2, I1-1, and I1-2, with active periods T8, T7-1 = T7-2 = T7/2, and T1-1 = T1-2 = T1/2, derived from vectors I8, I7, and I1. Similarly, in minor sector S3, vectors I1-1, I1-2, I6-1, I6-2, I7-1, and I7-2 are used, with active periods based on I1, I6, and I7. Table 2 lists all switching vectors per minor sector.

A switching sequence pattern for symmetric waveforms, minimal switch transitions, and balanced switch utilization is developed, as shown in Table 2.

The reference space vector is created by utilizing the nearest switching state vectors for a specific minor sector, such as I6-1, I1-4, and I7-2 in minor sector S17 and I7-2, I7-1, and I1-4 in minor sector S18.

Table 2: Sector-Based Switching State Vectors in Method 2

Major sector	Minor sector	Switching state vector position			Switching state vectors			Switching states sequence							Number of switch transitions								
		x	y	z	x	y	z	$\frac{T_z}{4}$	-	$\frac{T_x}{2}$	-	$\frac{T_y}{2}$	-	$\frac{T_z}{2}$	-	$\frac{T_x}{2}$	-	$\frac{T_y}{2}$	-	$\frac{T_z}{4}$	CFI-1	CFI-2	Total
	S <sub>1</sub>	I <sub>p</sub>	I <sub>q</sub>	I <sub>0</sub>	I <sub>p-1</sub> and I <sub>p-2</sub>	I <sub>q-1</sub> and I <sub>q-2</sub>	I <sub>0-0</sub>	(i <sub>m</sub> , i <sub>m</sub> )	-	(i <sub>p</sub> , i <sub>m</sub> )	-	(i <sub>q</sub> , i <sub>m</sub> )	-	(i <sub>m</sub> , i <sub>m</sub> )	-	(i <sub>m</sub> , i <sub>p</sub> )	-	(i <sub>m</sub> , i <sub>q</sub> )	-	(i <sub>m</sub> , i <sub>m</sub> )	6	6	12
	S <sub>2</sub>	I <sub>r</sub>	I <sub>s</sub>	I <sub>p</sub>	I <sub>r-1</sub> and I <sub>r-2</sub>	I <sub>p-1</sub> and I <sub>p-2</sub>	I <sub>r</sub>	(i <sub>p</sub> , i <sub>m</sub> )	-	(i <sub>p</sub> , i <sub>p</sub> )	-	(i <sub>q</sub> , i <sub>p</sub> )	-	(i <sub>m</sub> , i <sub>p</sub> )	-	(i <sub>p</sub> , i <sub>p</sub> )	-	(i <sub>p</sub> , i <sub>q</sub> )	-	(i <sub>p</sub> , i <sub>m</sub> )	6	6	12
S <sub>M</sub>	S <sub>3</sub>	I <sub>p</sub>	I <sub>q</sub>	I <sub>s</sub>	I <sub>p-1</sub> and I <sub>p-2</sub>	I <sub>q-1</sub> and I <sub>q-2</sub>	I <sub>s-1</sub> and I <sub>s-2</sub>	(i <sub>p</sub> , i <sub>q</sub> )	-	(i <sub>p</sub> , i <sub>m</sub> )	-	(i <sub>q</sub> , i <sub>m</sub> )	-	(i <sub>q</sub> , i <sub>p</sub> )	-	(i <sub>m</sub> , i <sub>p</sub> )	-	(i <sub>m</sub> , i <sub>q</sub> )	-	(i <sub>p</sub> , i <sub>q</sub> )	6	6	12
	S <sub>4</sub>	I <sub>s</sub>	I <sub>t</sub>	I <sub>q</sub>	I <sub>s-1</sub> and I <sub>s-2</sub>	I <sub>q-1</sub> and I <sub>q-2</sub>	I <sub>t</sub>	(i <sub>q</sub> , i <sub>m</sub> )	-	(i <sub>q</sub> , i <sub>p</sub> )	-	(i <sub>q</sub> , i <sub>q</sub> )	-	(i <sub>m</sub> , i <sub>q</sub> )	-	(i <sub>p</sub> , i <sub>q</sub> )	-	(i <sub>q</sub> , i <sub>q</sub> )	-	(i <sub>q</sub> , i <sub>m</sub> )	6	6	12

IV SIMULATION RESULTS

Method 1 shows that the current i<sub>a</sub>, which includes intermediate current levels, significantly reduces low-

frequency harmonic components, as shown in Fig. 5(a), and the Figures 5(b) and 5(c) phase-a current for CFI-1 and CFI-2.

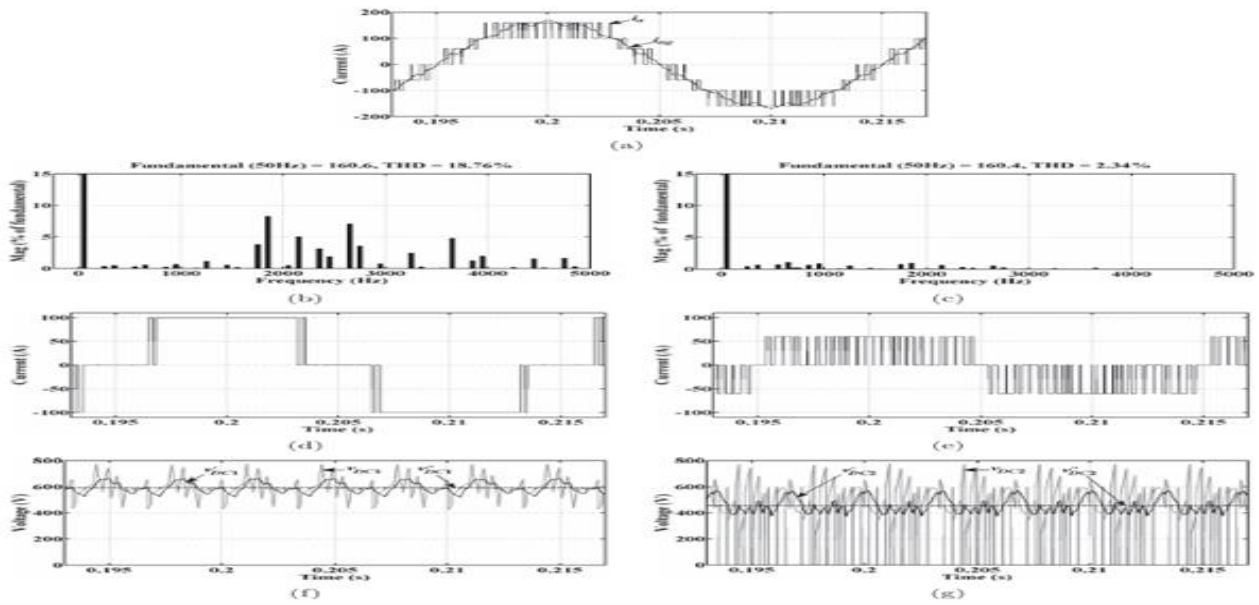


**Figure 5: Simulation Results for Method-1 with  $I_{dc1}=100$  A and  $I_{dc2}=60$  A: (a) Output Current  $I_a$  and Grid Current  $I_{ag}$  (b) Harmonic Spectrum of Output Current  $I_a$  (c) Harmonic Spectrum of Grid Current  $I_{ag}$  (d) Phase-A Current  $I_{a1}$  for CFI-1 (e) Phase-A Current  $I_{a2}$  for CFI-2 (f) DC-Link Voltage  $V_{dc1}$  for CFI-1 (g) DC-Link Voltage  $V_{dc2}$  for CFI-2**  
Method 2 selects specific switching state vectors to eliminate low-frequency pulsations in DC-link voltages of CFIs, stabilizing DC-link voltage for complex, high-performance inverter systems, as shown in simulation results. in fig. 6

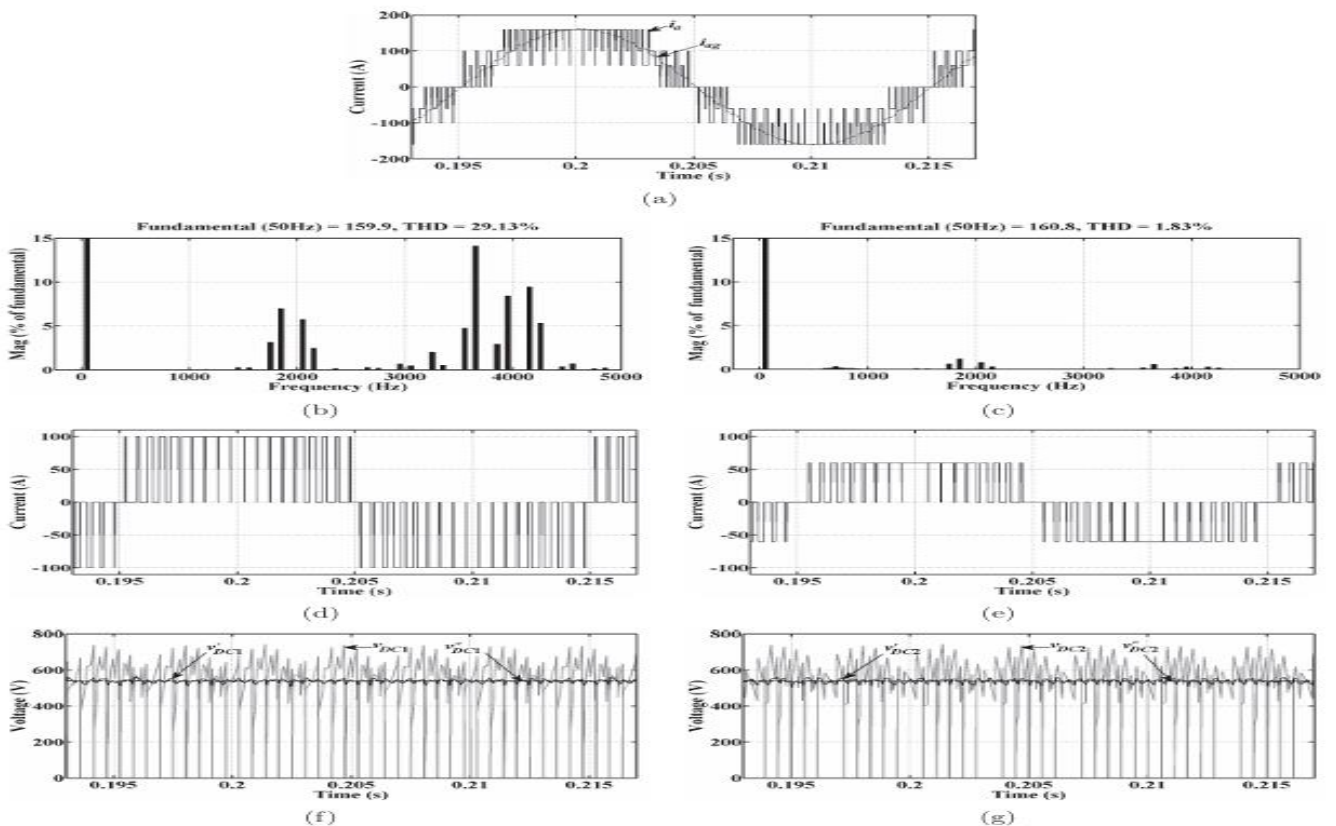


**Figure 6: Simulation results for Method-2:  $i_{DC1} = 100$  A and  $i_{DC2} = 60$  A (a) Output Current  $i_a$  and Grid Current  $i_{ag}$  (b) Harmonic Spectrum of Output Current  $i_a$  (c) Harmonic Spectrum of Grid Current  $i_{ag}$  (d) Phase-a Current  $i_{a1}$  for CFI-1 (e) Phase-a Current  $i_{a2}$  for CFI-2 (f) DC-link Voltage  $V_{DC1}$  for CFI-1 (g) DC-link Voltage  $V_{DC2}$  for CFI-2**



### V CONCLUSION

Two methods using SVM technique are used to select switching state vectors in multilevel current-fed inverters (CFIs) to eliminate low-frequency harmonic components in output currents, particularly under unequal dc-link current conditions.

Method 1 creates a reference current space vector using nearest switching state vectors in minor sectors, allowing higher current inverters to operate at lower frequencies, improving efficiency. However, this method has low-frequency pulsations in DC-link

voltage and requires careful design of DC-DC converters to accommodate output voltage variations due to inequality in DC-link currents.

Method 2 selects switching state vectors to eliminate low-frequency pulsations in CFI DC-link voltages, reducing computational burden and extending principles to systems with multiple parallel CFI units, and reduces the computational burden of identifying the operating sector and calculating duty cycles.

### VI REFERENCES

- [1] T. Noguchi, "Multilevel current waveform generation using inductor cells and H-bridge current-source inverter," IEEE Trans. Power Electron., vol. 27, no. 3, pp. 1090–1098, Mar. 2012.
- [2] M. P. Aguirre, L. Calvino, and M. I. Valla, "Multilevel current-source inverter with FPGA control," IEEE Trans. Ind. Electron., vol. 60, no. 1, pp. 3–10, Jan. 2013
- [3] R. B.S. Dupczak, A.J. Perin, and M.L. Heldwein, "Space vector modulation strategy applied to interphase transformers-based five-level current source inverters," IEEE Trans. Power Electron., vol. 27, no. 6, pp. 2740–2751, Jun. 2012..
- [4] S. Jian and W. L. Yun, "A space-vector modulation method for common mode voltage reduction in current-source converters," IEEE Trans. Power Electron., vol. 29, no. 1, pp. 374–385, Jan. 2014.
- [5] Z. Bai and Z. Zhang, "Conformation of multilevel current source converter topologies using the duality principle," IEEE Trans. Power Electron., vol. 23, no. 5, pp. 2260–2267, Sep. 2008
- [6] B. Mirafzal, M. Saghaleini, and A. Kaviani, "An SVPWM-based switching pattern for stand-alone and grid-connected three-phase single-stage boost inverters," IEEE Trans. Power Electron., vol. 26, no. 4, pp. 1102–1111, Apr. 2011.
- [7] Y. Suh, J. Steinke, and P. Steimer, "Efficiency comparison of voltage source and current-source drive systems for medium-voltage applications," IEEE Trans. Ind. Electron., vol. 54, no. 5, pp. 2521–2531, Oct. 2007.
- [8] V. Vekhande and B. G. Fernandes, "Module integrated DC-DC converter for integration of photovoltaic source with DC micro-grid," in Proc. IEEE Ind. Electron. Soc. Conf., IECON'2012, pp. 5657–5662, Oct. 2012.
- [9] c. Hanju, C. Jungwan and P. N. Enjeti, "A three-phase current-fed DC/DC converter with active clamp for low-DC renewable energy sources," IEEE Trans. Power Electron., vol. 23, no. 6, pp. 2784–2793, Nov. 2008

### BIOGRAPHIES

**G. Prem Kumar Reddy**, Presently Pursuing PhD in University College of Engineering, Osmania University, Hyderabad. His Completed M.Tech in Jawaharlal Nehru Technological University, Anantapur. His B.Tech Completed affiliated college of Jawaharlal Nehru Technological University, Hyderabad. His research interest on Multilevel Converter



**Dr. B. Mangu** was born in Warangal, India, in 1975. He received the B.E. and M.E. degrees from the University College of Engineering, Osmania University, Hyderabad, India, in 2000 and 2005, respectively. He received the Ph.D. degree with the Department of Electrical Engineering, IIT Bombay, Mumbai, India.

